Dynamic System Equivalents: A Survey of Available Techniques

IEEE PES General Systems Subcommittee—Task Force on Dynamic System Equivalents

U. D. Annakkage, *Senior Member, IEEE*, N. K. C. Nair, *Senior Member, IEEE*, Yuefeng Liang, *Student Member, IEEE*, A. M. Gole, *Fellow, IEEE*, V. Dinavahi, *Member, IEEE*, Bjorn Gustavsen, *Senior Member, IEEE*, Taku Noda, *Senior Member, IEEE*, Hassan Ghasemi, *Member, IEEE*, A. Monti, *Senior Member, IEEE*, Mah Matar, *Member, IEEE*, R. Iravani, *Fellow, IEEE*, and J. A. Martinez, *Member, IEEE*

***Abstract*—This paper presents a brief review of techniques available for reducing large systems to smaller equivalents. This paper is divided into high frequency equivalents, low frequency equivalents, and wideband equivalents. Numerical examples are presented to demonstrate selected methods of high frequency equivalencing.**

***Index Terms*—Coherency, dynamic equivalents, frequency-dependent network equivalents, modal analysis, two-layer network equivalents, vector fitting.**

I. Introduction

THERE are two commonly used power system simulation models: 1) electromagnetic transient (EMT) models, and 2) transient stability models or "phasor models." In EMT programs, power system components are adequately modelled to simulate high-frequency transients in power systems. This makes EMT programs very valuable in studies of lightning and switching overvoltages, and the effects of power-electronic devices on system behavior. In order to cover the necessary bandwidth, these programs use small integration time steps of the order of 50 μs or less, making EMT programs much slower than transient stability programs. On the other hand, stability programs, based on "phasor models" of transmission lines and simplified rotating machine models use a much larger integration time step (typically half a cycle) enabling such programs to solve large power systems in excess of 50 000 buses.

The common practice in dealing with large systems in EMT programs is to divide the system into a *study zone* where transient phenomena occur and an *external system* encompassing the rest of the system, in order to reduce computational burden. The generators in the external system are represented by power frequency voltage sources. This simplification eliminates electromechanical type low-frequency behavior from the model, and the resulting model is suitable for the simulation of lightning and switching overvoltages. In situations where power-electronic devices are used to mitigate low-frequency electromechanical oscillation problems in a power system, the high-frequency equivalent network representation for the external system is inadequate. Therefore, there is a need for developing suitable techniques to determine dynamic equivalent models that accurately represent the relevant low frequency as well as the high-frequency behavior of the external system.

The adequacy of the power system model depends on the transient or dynamic phenomena to be studied. This could be broadly classified into three categories: To investigate 1) high-frequency transients, where the transmission lines must be properly modelled to reflect the frequency-dependent effects; 2) for low-frequency electromechanical oscillation studies, where the transmission lines can be modelled as constant impedances and the generators can be modelled without stator winding transients; and 3) studies that involve subsynchronous oscillations, where both the turbine-generator dynamics and network transients must be adequately modelled. These three types of studies need three types of equivalents: high-frequency equivalents (HFE), low-frequency equivalents (LFE), and wideband equivalents, respectively. This paper is divided according to this classification. The discussion on the LFE is limited to the methods that are relevant to EMT analysis.

II. High-Frequency Equivalents (HFE)

A. Introduction

The HFEs can be further classified into frequency-dependent network equivalents (FDNE), and two-layer network equivalents (TLNE). Both of these methods attempt to model the frequency-dependent terminal admittance of a network using either a lumped parameter circuit model or a rational function model.

The modeling, which assumes linearity of the considered subsystem, is normally based on an admittance formulation which defines the relation between voltage V and currents I on the ports (terminals) of the equivalent

$$\mathbf{YV} = \mathbf{I}. \tag{1}$$

Manuscript received July 21, 2011; accepted August 04, 2011. Date of publication October 14, 2011; date of current version December 23, 2011. Paper no. TPWRD-00617-2011.

The authors are with the IEEE Power and Energy Society General Systems Subcommittee—Task Force on Dynamic System Equivalents (e-mail: annakkag@ee.umanitoba.ca).

Color versions of one or more of the figures in this paper are available online at http://ieeexplore.ieee.org.

Digital Object Identifier 10.1109/TPWRD.2011.2167351

B. Frequency-Dependent Network Equivalent (FDNE)

The known frequency response admittance characteristic of the external system can be estimated by fitting it to a function of the appropriate order

$$f_{\text{fit}}(s) = \frac{p_0 + p_1 s + p_2 s^2 + \cdots + p_N s^N}{1 + q_1 s + q_2 s^2 + \cdots + q_N s^N} \tag{2}$$

or the equivalent form

$$f(s) = c_0 + \sum_{k=1}^{N} \frac{c_k}{s - a_k}. \tag{3}$$

As measured or calculated values of $f(j\omega_p)$ are known at an arbitrarily large number of frequency points, (3) (or equivalently, (2)) can be expressed as an overdetermined fitting problem in the $2n + 1$ variables $a_1, a_2 \ldots a_N$, and $c_0, c_1, c_2 \ldots c_n$. However, this is a nonlinear problem that cannot be solved by well-known linear regression methods.

An early work reported in the literature used frequency domain computed data to fit parameters to the model in (2)[1].

References [2] and [3] overcome ill-conditioning problems of FDNE, by dividing the frequency response into sections. Other techniques, such as column scaling, adaptive weighting, and iterations step adjustment are also utilized in these references.

A time domain approach to obtain the fitted function (3) using Prony Analysis is presented in [4]. Time domain approaches have also been applied to identify the external system as a digital filter in [5] and [6]. In [7], [10], and [11], the external system is modelled using lumped parameters.

Recently, a more powerful *vector fitting technique* has been employed [12]–[14], [19], [20]. Vector fitting converts the problem in (2) into a linear problem as will be described. An unknown rational function of the form (4) is introduced with an initial pole set $d_1, d_2 \ldots d_N$

$$\sigma(s) = 1 + \sum_{k=1}^{N} \frac{b_k}{s - d_k}. \tag{4}$$

The function $\sigma(s)$ with yet-to-be-determined residues b_k is required to satisfy the condition (5) where the right side has the same poles as $\sigma(s)$. Since the poles in (5) are known, the equation is linear in its unknown residues and can therefore be solved as an overdetermined linear problem in the least-squares sense

$$f(s)\sigma(s) = e_0 + \sum_{k=1}^{N} \frac{e_k}{s - d_k}. \tag{5}$$

An improved pole set for the approximation of $f(s)$ is calculated as the zeros of σ, which are obtained by solving an eigenvalue problem (6)[12]. In (6), A is a diagonal matrix holding the initial poles $\{d_k\}$, b is a column vector of ones, and c^T is a row vector holding the residues $\{e_k\}$

$$a_m = eig(A - bc^T). \tag{6}$$

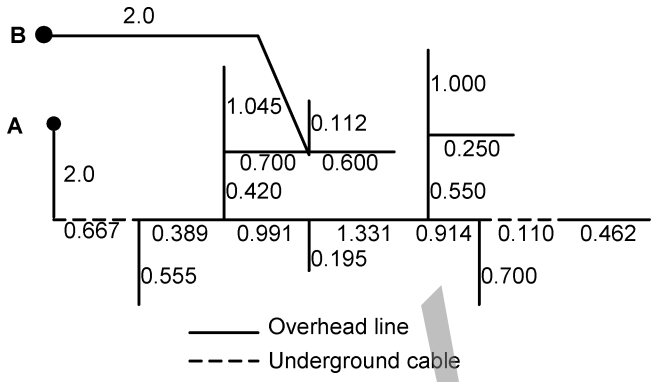

Fig. 1. Topology of the distribution test system (lengths in kilometers).

This procedure is applied in an iterative manner where (5) and (6) are solved repeatedly with the new poles replacing the previous poles $\{d_k\}$. This pole relocation procedure usually converges in 3–5 iterations. After the poles have been identified, the residues of (3) are finally calculated by solving the corresponding least-squares problem with known poles.

The fitting process works better when the arbitrarily assigned poles d_k of $\sigma(s)$ are close to the poles c_k of $f(s)$. Hence, although one pass through the procedure should be sufficient, using the values of c_k determined through an earlier iteration as seed values d_k for the next iteration can yield improved fitting. Additional care is required to ensure that the fitted function is stable and passive.

Most practical applications involve one or more three-phase buses. In such multiport cases, the same modeling procedure is applicable as vector fitting can be applied to several elements simultaneously. In practice, one stacks the elements of Y into a single vector and subjects it to vector fitting which produces a rational model with a common pole set, which after rearrangement of fitting parameters, gives the pole-residue model (7). A symmetrical model is obtained by fitting only the upper (or lower) triangle of Y

$$Y = \sum_{k=1}^{N} \frac{R_k}{s - a_k} + R_0. \tag{7}$$

1) Example on High-Frequency FDNE:

Modeling: This example taken from [8] demonstrates how to calculate a high-frequency FDNE (HFDNE) for the distribution system in Fig. 1 with respect to the two three-phase buses A and B. The admittance matrix with respect to these buses is established via the nodal admittance matrix where each branch (line/cable) is represented by its exact PI-equivalent in phase domain coordinates. Using vector fitting and passivity enforcement, a rational model is obtained in the frequency range 10 Hz to 100 kHz, see Fig. 2. The model has 60 pole-residue terms.

Time Domain Simulation: The model is included in the PSCAD/EMTDC circuit simulator via a user-defined component. In a time domain simulation, bus A is energized from a three-phase voltage source with bus B being open. At $\mathrm{t} = 20$ ms, a ground fault occurs at A3, see Fig. 3. The voltage response at B3 is simulated in PSCAD/EMTDC in two alternative ways:

1) using HFDNE;

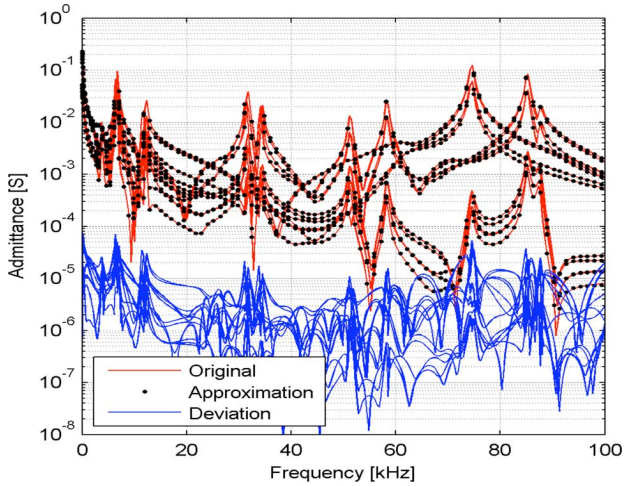

Fig. 2. Rational fitting of Y (6?6) (depicted from [8]).

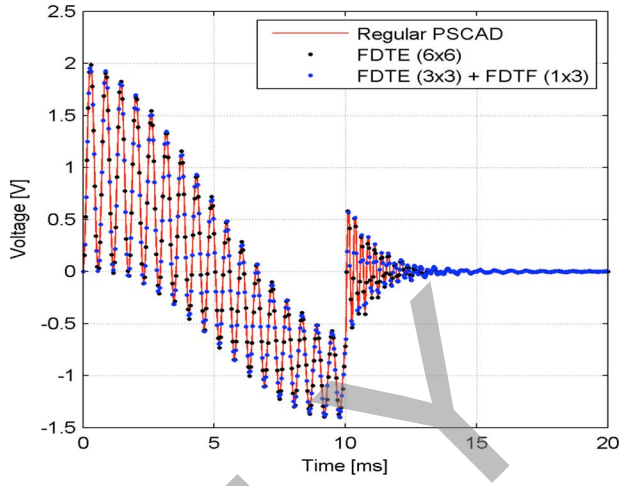

Fig. 4. Transient voltage on B3 (depicted from [8]). FDTF stands for the frequency-dependent transfer function model and FDTE stands for the frequency-dependent terminal equivalent.

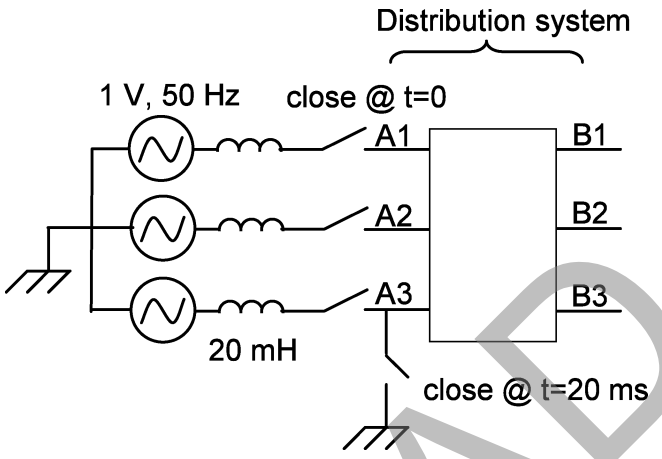

Fig. 3. Energization and ground fault initiation (depicted from [8]).

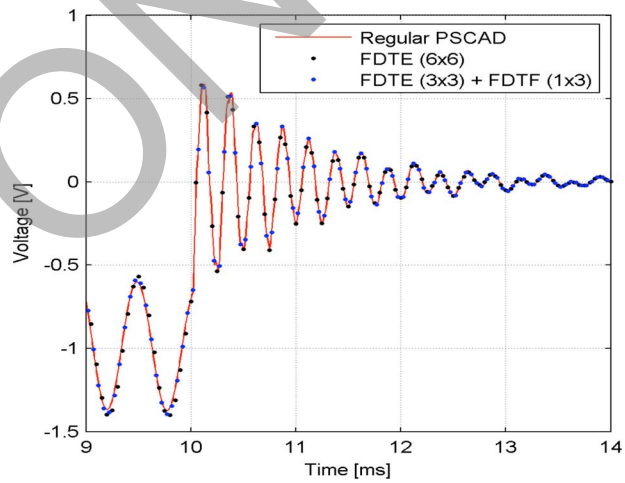

Fig. 5. Transient voltage on B3 (expanded view) (depicted from [8]), FDTF stands for frequency-dependent transfer function model and FDTE stands for frequency-dependent terminal equivalent.

2) standard simulation with all lines/cables explicitly represented by the universal line model [9] .

Figs. 4 and 5 show the voltage response on B3 with the two alternative simulation procedures. The responses by the two approaches are seen to match very closely. The computation time by the HFDNE can be made much smaller than that by the full model [8]. With the full model, the time step must be kept smaller than 0.2 μs due to the presence of small stub lines, since the traveling-wave method requires the time step to be smaller than the time delay of all lines. With the HFDNE, however, a larger time step is permissible. This gives large savings in computation time [8].

Partitioning the Frequency Response: This example was taken from [2] to demonstrate the effectiveness of partitioning the frequency response. The test system shown in Fig. 6 is a three-phase, 500-kV transmission network. Fig. 7(a) shows the equivalent circuit for the generators G 1–4. The electromotive forces (emfs) are represented by the three-phase sinusoidal voltage source E, and the subtransient impedance by the circuit block consisting of L_1, R_2, and L_2. Fig. 7(b) is the equivalent circuit used to represent the transformers TR 1–4, consisting of the $\Delta - Y$ ideal transformer and the $L_1 - R_2 - L_2$ circuit block. This circuit block represents the frequency dependence of the leakage impedances of the transformers. The loads LD 1–6 are modeled by the simple $R - L$ circuit in Fig. 7(c). As in Fig. 7(d), the capacitor bank consists of the delta-connected capacitors and the step-down transformer. The step-down transformer is represented in the same way as TR 1–4, and the stray capacitance to the ground is considered by the 1-nF capacitances. Refer to [2] for details of the transmission-line model.

The admittance matrix $\mathbf{Y}(s)$ of the test network's external zone is calculated at equidistant 2000 frequency points between 0 Hz and 10 kHz. The trace of $\mathbf{Y}(s)$ is then calculated and partitioned into ten frequency sections as shown in Fig. 8 Each partition of the trace is fitted by the rational fitting method described in [2]. Fig. 9 shows the fitted result, where only some elements of the admittance matrix are shown, but the other elements are also fitted with the same degree of accuracy. The responses have

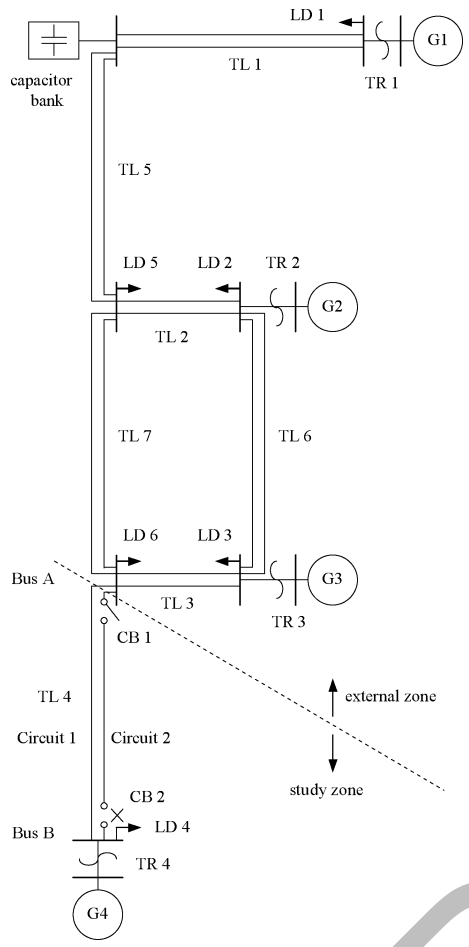

Fig. 6. The 500-kV test network.

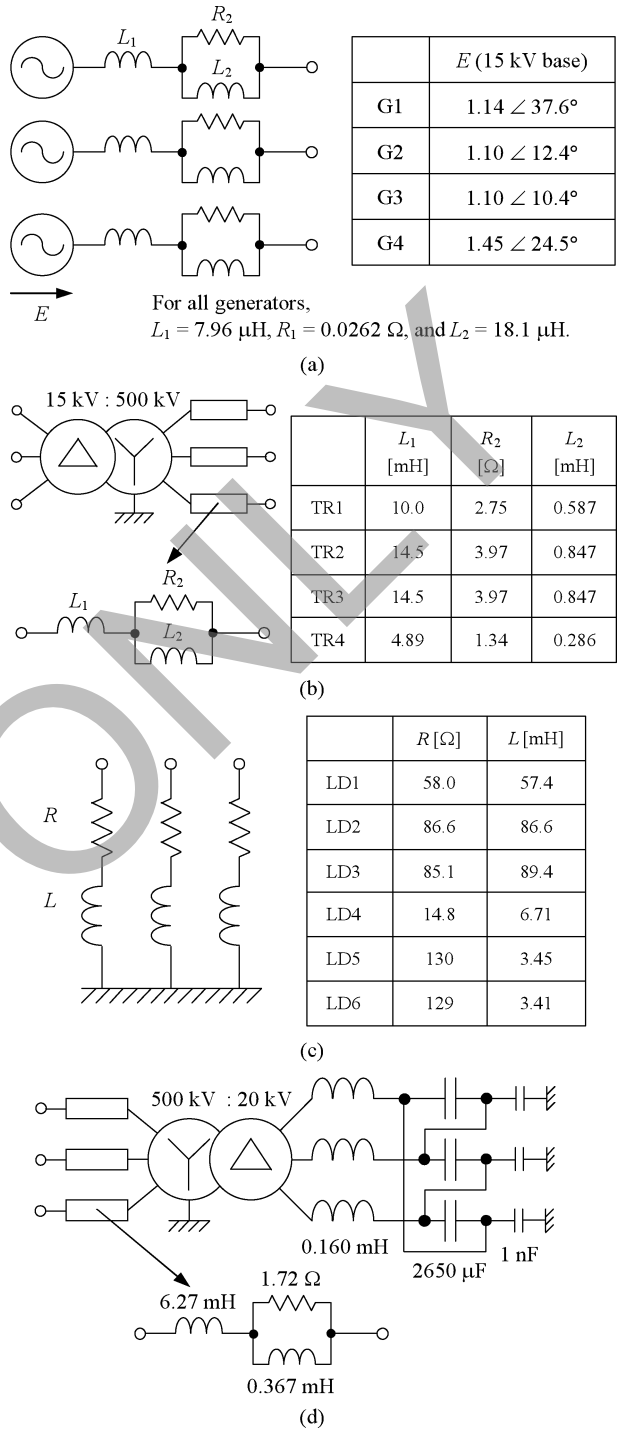

	E (15 kV base)
G1	1.14 ∠ 37.6°
G2	1.10 ∠ 12.4°
G3	1.10 ∠ 10.4°
G4	1.45 ∠ 24.5°

	L_1 [mH]	R_2 [Ω]	L_2 [mH]
TR1	10.0	2.75	0.587
TR2	14.5	3.97	0.847
TR3	14.5	3.97	0.847
TR4	4.89	1.34	0.286

	R [Ω]	L [mH]
LD1	58.0	57.4
LD2	86.6	86.6
LD3	85.1	89.4
LD4	14.8	6.71
LD5	130	3.45
LD6	129	3.41

Fig. 7. Representations of the network components. (a) Generator representation. (b) Transformer representation. (c) Load representation. (d) Capacitor bank representation.

many resonance peaks mainly due to the transmission lines, and all of those peaks are fitted accurately.

The switching transient due to closing the CB 1 at 7.09 ms is shown in Fig. 10. It compares the calculated voltages at CB 2 obtained by the full system representation and by the identified equivalent, where these results are practically the same.

C. Two-Layer Network Equivalent (TLNE)

In large systems, the complexities of an external system result in a high-order rational function (matrix), which requires excessive computations in transient simulations. This is not only an obstacle in offline simulation, but also the main bottleneck in achieving real-time simulation of realistic size power systems. The TLNE [22]–[24] in which the external system is further partitioned (Fig. 11) into a surface layer comprised of low-order frequency-dependent transmission lines and a deep region composed of low-order FDNE model, overcomes this obstacle. The contribution of the surface layer and deep region on the external system input admittance varies with frequency. In particular, the surface layer and deep region have effects on the admittance at low frequency. However, since transients in the study zone do not travel very far in external systems, the deep region mainly contributes to the lower frequency range, while the high-frequency characteristics of the external system are predominantly determined by the surface-layer transmission lines immediately connected to the study zone. Both the surface layer and deep region parameters can be further optimized in terms of their accuracy and efficiency in order to achieve a Robust TLNE [24] for real-time simulation. An application of the Robust TLNE for real-time transient simulation of large-scale systems on a PC-cluster-based real-time simulator is shown in [31]. The concept similar to this has been applied in [30] where the time delay in a transmission line, which connects the external system and the study zone, is used to perform the necessary calculations to

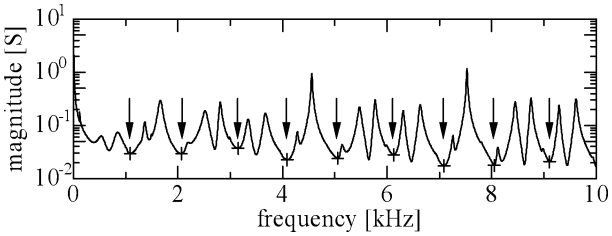

Fig. 8. Frequency response (magnitude) of the trace of the test network's admittance matrix and its partitioning. The response is partitioned into ten frequency sections, and the boundaries are marked as by the "+" symbols.

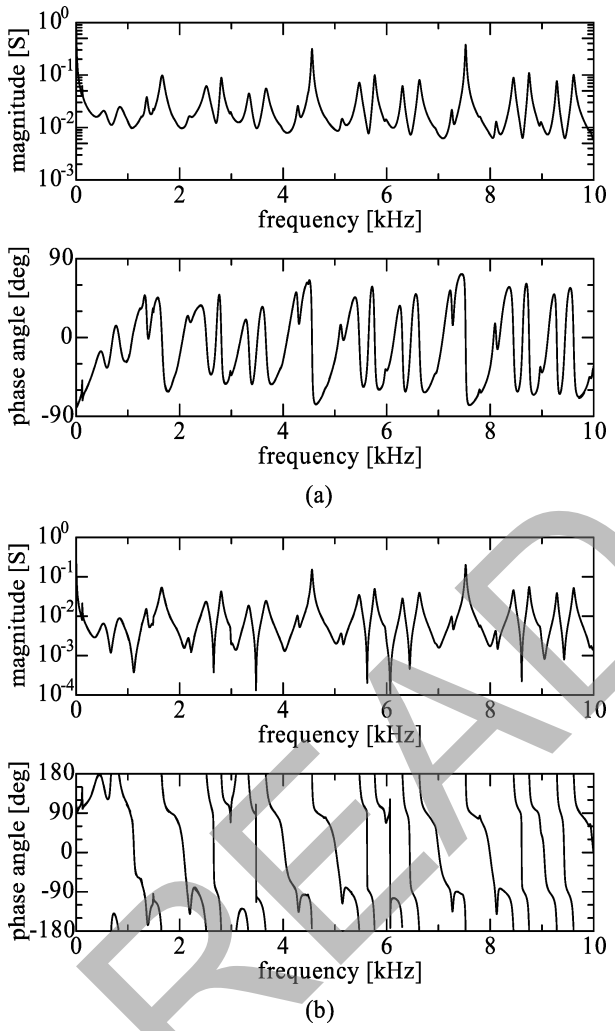

Fig. 9. Fitted result for some elements of the admittance matrix. (a) (1,1) element. (b) (1,2) element. The given responses are shown by the solid lines. The fitted responses are superimposed with the dashed lines and the difference from the solid lines cannot be observed.

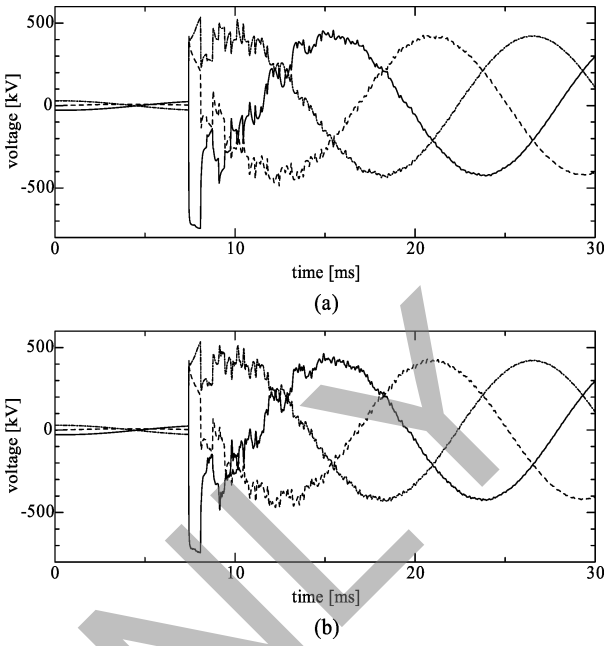

Fig. 10. Switching transient simulation results by (a) the full system representation and (b) the identified equivalent. (Solid line: phase a, dashed line: phase b, and dahs-dot line: phase c).

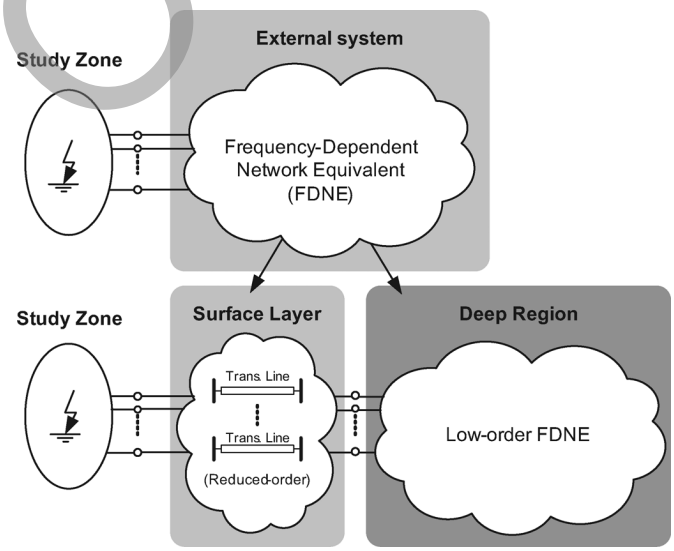

Fig. 11. Two-layer network equivalent (TLNE) concept [24].

interface the frequency domain model of the external system to the study zone. The frequency domain model of the external system is obtained by performing Fourier transform over the time domain data collected over a period of 2τ, where τ is the wave travel delay in the transmission line.

The passivity criterion has a strong impact on the stability of time-domain simulations; an electric network with passivity violations will result in unstable and erroneous simulations. For a network represented by the nodal (1), the passivity criterion requires that the real part of the input admittance $\mathbf{Y}$ be positive at all frequencies for a single-port network, or all eigenvalues of the real part of the input admittance matrix $\mathbf{Y}$ be positive in the entire frequency range for a multiport network.

In the TLNE method, the approximations of surface layer admittance $\mathbf{Y}_{surface}(\omega)$ and deep region admittance $\mathbf{Y}_{deep}(\omega)$ are obtained from low-order vector fitting [12]. Then, the input admittance $\mathbf{Y}_{input}(\omega)$ of the external system is obtained by combining $\mathbf{Y}_{\mathrm{surface}}(\omega)$ and $\mathbf{Y}_{\mathrm{deep}}(\omega)$ as shown in Fig. 12.

In the robust TLNE, GAs are used to find out the best low-order deep region $\mathbf{Y}_{\mathrm{deep}}(\omega)$ approximation which can minimize the deviation of external system input admittance $\mathbf{Y}_{\mathrm{input}}(\omega)$ approximation. Further improvement is achieved by the constrained nonlinear least-square optimization with the inclusion

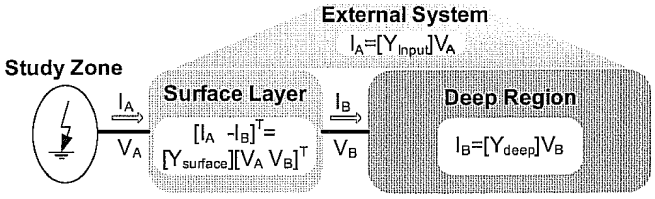

Fig. 12. Admittance matrix construction for the TLNE external system [24].

of frequency response at dc and the optimal deep region order determination feature.

1) Surface Layer: The surface layer consists of reduced-order frequency-dependent transmission-line models. In the robust TLNE model, Marti's frequency-dependent line model [32] is employed for real-time implementation. It is based on the well-known line model equations in the frequency domain

$$V_k(\omega) = \cosh[\gamma(\omega)\ell]V_m(\omega) - Z_c(\omega)\sinh[\gamma(\omega)\ell]I_m(\omega) \quad (8a)$$

$$I_k(\omega) = \frac{1}{Z_c(\omega)}\sinh[\gamma(\omega)\ell]V_m(\omega) - \cosh[\gamma(\omega)\ell]I_m(\omega) \quad (8b)$$

where $V_k(\omega)$, $V_m(\omega)$, $I_k(\omega)$, and $I_m(\omega)$ are the voltages and currents corresponding to the sending end (k) and receiving end (m), respectively; ℓ is the line length; and $Z_c(\omega)$ and $\gamma(\omega)$ are the frequency-dependent characteristic impedance and propagation function, respectively.

From individual lines, which have the nodal equations (8a) and (8b), the admittance matrix of the reduced-order surface-layer network can be constructed as follows:

$$\tilde{\mathbf{Y}}_{\text{surface}}(\omega) = \begin{bmatrix} \tilde{\mathbf{Y}}_{AA}(\omega) & \tilde{\mathbf{Y}}_{AB}(\omega) \\ \tilde{\mathbf{Y}}_{\text{BA}}(\omega) & \tilde{\mathbf{Y}}_{\text{BB}}(\omega) \end{bmatrix} \quad (9)$$

where subscript $_A$ stands for the ports connected to the study zone, subscript $_B$ stands for the ports connected to the deep region (Fig. 12), and $\tilde{}$ designates an approximation.

2) Deep Region: The fitting of the external system by vector fitting is stressed on a relatively lower frequency range since high-frequency transients do not travel very far in the external system. In the TLNE, the deep region is further insulated from the study zone by the surface layer. Thus, the order of the deep region can be significantly reduced.

The first approximation of external system input admittance $\tilde{\mathbf{Y}}^0_{\text{input}}(\omega)$ is the initial mathematical combination of admittance matrix $\tilde{\mathbf{Y}}_{\text{surface}}(\omega)$ of the surface layer constituting reduced-order line models and $\tilde{\mathbf{Y}}_{deep}(\omega)$ of the Deep Region comprising low-order FDNE

$$\tilde{\mathbf{Y}}^0_{\text{input}}(\omega) = \tilde{\mathbf{Y}}^0_{AA}(\omega) - \tilde{\mathbf{Y}}^0_{\text{AB}}(\omega) * [\tilde{\mathbf{Y}}^0_{BB}(\omega) + \tilde{\mathbf{Y}}^0_{deep}(\omega)]^{-1}\tilde{\mathbf{Y}}^0_{BA}(\omega) \quad (10)$$

where the superscript ^{0} denotes "first" since the subsequent optimizations are to be carried out, and $\tilde{\mathbf{Y}}^0_{AA}(\omega)$, $\tilde{\mathbf{Y}}^0_{AB}(\omega)$, $\tilde{\mathbf{Y}}^0_{BA}(\omega)$, and $\tilde{\mathbf{Y}}^0_{BB}(\omega)$ correspond to the blocks of the first approximation of surface layer admittance $\tilde{\mathbf{Y}}^0_{surface}(\omega)$ in (9). The ultimate goal of building the robust TLNE is to match $\tilde{\mathbf{Y}}_{\text{input}}(\omega)$ with the original external system input admittance $\mathbf{Y}_{\text{input}}(\omega)$ as close as possible while ensuring stability and passivity of the model, and accurate frequency response at dc and power frequency.

Since genetic algorithms try to find out the best low-order deep region $\tilde{\mathbf{Y}}^0_{\text{deep}}(\omega)$ that minimizes the difference between $\tilde{\mathbf{Y}}^0_{\text{input}}(\omega)$ and $\mathbf{Y}_{\text{input}}(\omega)$ while ensuring $\tilde{\mathbf{Y}}^0_{deep}(\omega)$ is positive-real, the objective function for a m-port external system is defined as follows:

$$f_{\text{obj}} = \left\| \mathbf{Y}_{\text{input}}(\omega) - \tilde{\mathbf{Y}}^0_{\text{input}}(\omega) \right\|_F^2 + \mu = \sum_{i,j=1}^{m} \left| \mathbf{Y}_{\text{input,ij}}(\omega) - \tilde{\mathbf{Y}}^0_{\text{input,ij}}(\omega) \right|^2 + \mu \quad (11)$$

where $\mathbf{Y}_{ij}(\omega)$ is the ijth element of the matrix $\mathbf{Y}(\omega)$; μ denotes a penalty term when the passivity criterion violation occurs in the deep region. If the criterion is violated, μ will be a large positive number, or else $\mu = 0$. This ensures that the outputs from GAs are the best-fitted deep regions, which are both stable and positive-real.

The complete flowchart of the robust TLNE procedure is given in [24]. This method was employed to derive an accurate frequency-dependent network equivalent of the 240-kV backbone network of the Alberta Interconnected Electric System (AIES), and used in real-time transient simulations which were validated using offline simulations with full system representation.

D. Modified Two-Layer Network Equivalent (M-TLNE)

The modified TLNE (M-TLNE) developed in [25] is an effort to further enhance the computational efficiency of the TLNE. The M-TLNE focuses on the surface region of the TLNE and significantly reduces its order. The model for the transmission lines in the surface layer is further simplified by representing the characteristic impedance as a constant resistance rather than by a frequency-dependent rational function. The adverse impact of this simplification, which mainly shows up in the frequency response of the equivalent, approximately within 0–150 Hz, is overcome by adding a first-order rational function to the input port of the M-TLNE. Thus, in the M-TLNE, the surface layer is approximated with a set of low-order transmission lines and a first-order rational function connected at the interface port of the equivalent, whereas the deep region is approximated with a low-order rational function. Fig. 13 shows a schematic of the proposed M-TLNE equivalent.

Although the schematic of the proposed M-TLNE (Fig. 13) appears more complicated than that of the original TLNE, the transmission-line model used in the M-TLNE is significantly simpler than the one used in the original TLNE.

A transmission line is characterized by two frequency-dependent functions: a propagation function H_p and a characteristic impedance Z_c[26]–[28]. The propagation function H_p defines the relationship between the reflected wave at one end of the line and the incident wave at the other end

$$H_p = e^{-\gamma\ell} \quad (12)$$

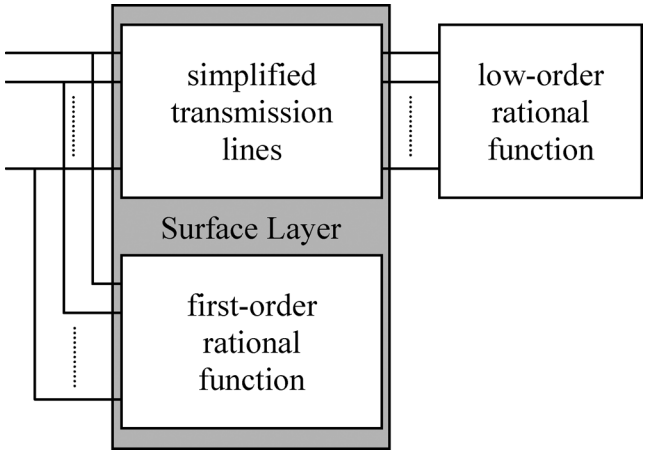

Fig. 13. Conceptual representation of the M-TLNE.

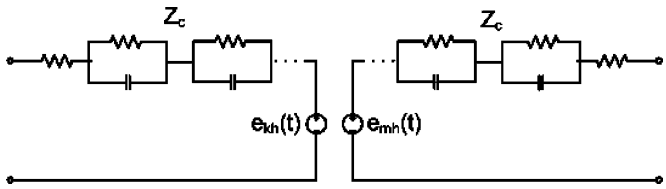

Fig. 14. Frequency-dependent transmission-line model.

where γ is the propagation constant and ℓ is the line length. H_p can be decomposed into a delay component H_o and a shaping component H_{sh}

$$H_p = H_o H_{sh}, \tag{13}$$

where H_{sh} is extracted from the propagation function through its multiplication by $\mathrm{e}^{j\varpi\tau}$, and approximated by a low-order rational function (e.g., using vector fitting (VF) [13]). The shaping function is approximated as a strictly proper rational function.

The characteristic impedance is approximated as the sum of partial fractions in the form of

$$Z_c = R_c + \sum_{i=1}^{n} \frac{r_i}{s + p_i}. \tag{14}$$

Usually, a 4th- to 6th-order rational function is used to model the frequency dependence of Z_c.

Fig. 14 shows the transmission-line model, including the frequency dependence of the characteristic impedance [28]. The frequency dependence of Z_c can only be neglected if the transmission line is open ended; otherwise, it results in deviation in the frequency response [28]. The deviation caused by neglecting the frequency dependence of Z_c is mainly in the low-frequency region (i.e., 0 to 150 Hz). In the M-TLNE, this deviation is effectively compensated by a first-order rational function connected at the input port of the transmission-line model. Thus, in the time domain model of the proposed M-TLNE, these RC blocks are discarded and only a fixed resistance is used to represent Z_c at each segment of the line model.

The merits of such a simplification are more pronounced when a multiphase multiport system is considered and the surface layer has a number of transmission lines. Thus, elimination of the RC blocks (Fig. 14) significantly reduces the number of equations required for the time-domain simulation model and, thus, noticeably reduces the computation time, particularly when the model is intended for real-time simulation.

The first approximation of the M-TLNE is constructed by connecting the approximated surface layer and the approximated deep region together. The input admittance of the first approximation is close to the original input admittance. However, the parameters of the equivalent need to be fine tuned to minimize deviations between the M-TLNE and the original network input admittance. The initial approximation provides a starting point to initiate the optimization process. The optimization can be achieved based on a least square process, with the objective function

$$O = \left\| Y_{\text{input}} - \tilde{Y}_{\text{input}} \right\|^2. \tag{15}$$

All of the parameters of the equivalent, either in the surface layer or in the deep region, are subject to optimization.

In comparison with the conventional TLNE, the M-TLNE adopts a simpler surface-layer model and, thus, reduces computation time. This is a salient feature when real-time and statistical time-domain simulation studies are of interest. The generalized methodology for developing the M-TLNE, along with several case studies of single- and multi-port systems, are presented in [25]. Reference [29] presents an implementation methodology for the M-TLNE in a field-programmable gate-array (FPGA)-based real-time power system simulator.

E. Other Methods

In [33] and [34], the time delay in a transmission line is used to interface the EMT model of the study zone with the transient stability model (low-frequency model) of the external system.

Different approaches have also been proposed that try to find a compromise for the dichotomy between time and frequency analysis. The concept of dynamic phasors has been applied in [35] and [36] to allow the use of a larger time step of integration than that used in EMT simulations. Basically, dynamic phasors provide a dynamic model for the dominant Fourier components of a signal assuming a sliding window of time. The resulting model is a state-space model representation where the state variables are time-variant Fourier components of the signal.

F. Numerical Issues

1) Accuracy Issues: When the terminals of the HFE include more than a single three-phase bus, the modeling becomes more challenging as error magnification problems may arise. When applying a voltage source to one bus, the model is required to produce large short-circuit currents with a short circuit applied to the other bus, and small currents if the second bus is open (charging currents). This behavior is reflected in the admittance matrix Y by large and small eigenvalues, respectively. Direct fitting of the elements of Y may easily result in corruption of its small eigenvalues, which may lead to error magnification with certain terminal conditions [21]. Some approaches, such as modal vector fitting [21], overcome this problem by assigning high weights to the small eigenvalues of Y in the least-squares fitting process.

2) Passivity: One major difficulty with rational function-based models is unstable simulation results due to passivity violations. Loss of passivity implies that the model can generate power under certain terminal conditions. A model is passive iff its nodal admittance matrix satisfies the passivity criterion [15].

$$\mathrm{eig}(Y + Y^H) > 0. \tag{16}$$

The passivity of the model can be checked by assessing the eigenvalues in (16) over a set of discrete frequency samples. In the case of rational models, the boundary frequencies of passivity violations can be checked by assessing the eigenvalues of a Hamiltonian matrix that is established directly from the models' state-space matrices [16]. In the case of symmetrical models, half-size matrices can be applied. The passivity can then be enforced by perturbing parameters of the model. Most commonly, this is done by perturbing the residues [17]–[19].

3) Transmission-Line Delay Effects: In many applications, the FDNE contains long transmission lines. The representation of time delays in the FDNE may require using an excessively high order with a pure rational model if the fitting has to be done over a wide frequency band. In these cases, the two-layer FDNE is particularly useful since it can greatly reduce the required order of the inner layer.

III. Low-Frequency Equivalents

A. Introduction

These models are used in simulating transient rotor-angle stability of synchronous machines (transient stability simulation). Most of the research efforts in this area were in the 1970s and 1980s when the computing power was dramatically less than today. The current industry practice is to simulate the full model due to the availability of fast computers. Despite the availability of fast computers, the need for low-frequency equivalents is still relevant when the influence of power-electronics devices on low-frequency oscillations is simulated using EMT-type simulations.

A vast amount of research has been done on the topic of LFEs. There is no intention to cover this topic in depth in this paper. Instead, the major branches of the research that are relevant to EMT analysis are briefly outlined.

For transient stability simulation, the dynamics of the generators and their auxiliary controllers are modelled as nonlinear differential equations. The transients in the network are typically at high frequency and highly damped. Therefore, the voltage and current relationships are modelled by using algebraic equations. This allows the currents and voltages I and V to be modelled in rms quantities and the network to be modelled with the admittance matrix $[Y]$ calculated at constant frequency. This gives differential and algebraic equations (DAE) for the kth generator (including auxiliary controllers) in the form given as

$$\dot{X}_k = f(X_k, V_k, u_k) \tag{17}$$

$$I_k = g(X_k, V_k) \tag{18}$$

and the network equations in the form of nodal equations (1).

The main interest in low-frequency equivalents is to model the electromechanical oscillation modes which are typically in the range of 0–2 *Hz*. These oscillations are relatively less damped. The purpose of equivalencing is to reduce the computing time. This can be achieved by reducing the number of generators and the network nodes. Alternatively, the dimension of the problem can be reduced by extracting only the relevant modes of oscillation from the dynamic model.

There are three main approaches reported in the literature:

1) modal methods where the external system is represented by an approximate linear model;
2) coherency methods where coherent groups of generators are identified and the generators in coherent groups are represented by an equivalent generator;
3) measurement or simulation-based methods where the external system response is either measured or simulated and curve-fitting techniques are used to determine the model parameters.

Some methods are combinations of the three.

B. Modal Methods

Modal methods are based on the linearized state-space model (19), derived from (1), (17), and (18)

$$[\dot{X}] = [A][X] + [B][u]. \tag{19}$$

Eigenvalues of the system matrix $[A]$ give the modes of the dynamic system. The complex conjugate eigenvalues give oscillatory modes, and the real eigenvalues give nonoscillatory modes.

When a system undergoes a transient subsequent to a disturbance, the oscillation modes with high damping decay faster than the modes with lower damping. Modal methods try to extract the relatively less damped modes (represented by eigenvalues of $[A]$ which are closer to the origin) and remove the highly damped modes (represented by eigenvalues of $[A]$ which are the farthest away from the origin). The relatively less damped modes are present in the responses over a longer period and, hence, determine the overall response [37]–[45].

A comprehensive framework known as selective modal analysis (SMA) for the analysis of selected parts of linear dynamic systems is presented in [40]–[42]. The method employs the eigenvalues, eigenvectors, and participation factors of the linear system to reduce the less relevant part of the network.

Modal methods have also been used to supplement the coherency methods where coherent groups are identified using modal methods [46]. A special class of modal methods is the structure preserving techniques where the zero entries of the device matrices are still retained as zero entries in the equivalent system matrix [47], [48].

C. Coherency Methods

In coherency methods [49]–[52], coherent groupings of machines are obtained by analyzing the system response to a perturbation. An equivalent of the external system is then obtained by replacing each such coherent group of machines by a large equivalent machine. Unlike the modal method, this approach retains the physical models of the generators in an equivalent form. The equivalent generator models are nonlinear. Coherency methods involve the following steps:

Step 1) identification of the groups of coherent generators;
Step 2) aggregation of the generator busses;

Step 3) aggregation of generator models and their associated control devices. [48], [49], [53];

Step 4) reduction of load buses.

An application of coherency-based dynamic reduction to a large power system using the DYNRED program developed by EPRI [54] is reported in [55]. In [56], coherency identification is performed by using the eigenvectors of the system matrix $[A]$ in (19). The method is based on the identification of a slow eigenbasis matrix corresponding to the electromechanical model of the power system (i.e., only the swing equations are modelled in (19)). The r number of the most linearly independent rows of the eigenbasis matrix become the corresponding reference generators. A grouping algorithm is then applied to group nonreference generators to reference generators. Finally, an eigenvector method is used to include load buses into coherent areas. This approach is referred to as the two time scale method because it is based on the separation of system dynamics to fast and slow modes [39]. A combination of a modal and coherency methods is presented in [57] and [58].

D. Measurement or Simulation-Based Methods

Measurement or simulation-based techniques use either real-time measurements or simulated responses of the power system. System identification techniques are used to identify the parameters of an equivalent model [59]–[62].

In [59], parameter identification is carried out using a least-squares algorithm with an adaptive step-size scheme. To start with, an equivalent model is first estimated. It is re-evaluated against the original system until the cost function has reached the minimum and all equivalent parameters have been identified. A similar principle is suggested in [60] and [61]. The main attempt here is to search for the best parameter vector which minimizes an error index that is taken to be a square function of the difference between the measured output and the calculated output. In [62], recorded disturbances are analyzed, equivalent parameters are identified, and then applied in dynamic simulations.

IV. Wideband Equivalents

Unlike the high-frequency and low-frequency equivalent models, which are valid in specific frequency ranges, wideband system equivalents model the behavior of the equivalenced external system over the entire frequency spectrum ranging from sub-Hertz electromechanical phenomena to several tens or hundreds of kilohertz electromagnetic phenomena. These tools are particularly of interest in real-time simulators. Real-time digital simulators are real-time implementations of EMT-type simulation on a parallel computation platform. Using these tools, a wideband EMT model of a power system with up to several hundred buses can be simulated in real time [63]. Since the simulation can be kept running continuously (over hours or days), in real time, it becomes possible to use the same tool for the study of very low- and high-frequency system behaviors. However, the size of the real-time hardware (counted in terms of processor racks) and, subsequently, its monetary cost is proportional to the size of the modelled system. Hence, it makes economic sense to model in full nonlinear detail only that part of the network which is of great interest (referred to as the internal system), and formulate the remainder (external system) of the network into an appropriately accurate equivalent. It should be noted that the equivalent must be able to properly represent the high-frequency electromagnetic as well as the low-frequency electromechanical transient behavior.

The implementation of wideband equivalents in a real-time environment has been reported in [63] and [64]. This method uses a multiport FDNE to represent the high-frequency behavior and uses a specially adapted real-time transient stability (TSA) simulator to calculate the lower frequency behavior.

V. Conclusions

A brief review of techniques available for obtaining dynamic system equivalents has been presented in this paper. The need for equivalent models has been driven by the demand for fast and accurate simulation tools. For EMT simulations, large networks need to be modelled using equivalent network models that accurately represent the high-frequency response of the original network. The generators are represented by voltage sources in these studies. For transient stability simulations, the high-frequency response is not important. The system reduction is achieved by grouping the generators together and eliminating the load buses to reduce the size of the network. The transmission network is modelled as constant impedances calculated at the power frequency. Wideband models that accurately model the high-frequency as well as low-frequency response are required in some applications of real-time simulation.

References

[1] A. O. Soysal and A. Semlyen, "Practical transfer function estimation and its application to wide frequency range representation of transformers," *IEEE Trans. Power Del.*, vol. 8, no. 3, pp. 1627–1637, Jul. 1993.

[2] T. Noda, "Identification of a multiphase network equivalent for electromagnetic transient calculations using partitioned frequency response," *IEEE Trans. Power Del.*, vol. 20, no. 2, pt. 1, pp. 1134–1142, Apr. 2005.

[3] T. Noda, "A binary frequency-region partitioning algorithm for the identification of a multiphase network equivalent for EMT studies," *IEEE Trans. Power Del.*, vol. 22, no. 2, pp. 1257–1258, Apr. 2007.

[4] J. Hong and J. Park, "A time-domain approach to transmission network equivalents via Prony analysis for electromagnetic transients analysis," *IEEE Trans. Power Syst.*, vol. 10, no. 4, pp. 1789–1797, Nov. 1995.

[5] H. Singh and A. Abur, "Multiport equivalencing of external systems for simulation of switching transients," *IEEE Trans. Power Del.*, vol. 10, no. 1, pp. 374–382, Jan. 1995.

[6] A. Abur and H. Singh, "Time domain modelling of external systems for electromagnetic transients programs," *IEEE Trans. Power Syst.*, vol. 8, no. 2, pp. 671–679, May 1993.

[7] A. S. Morched, J. H. Ottevangers, and L. Marti, "Multi-port frequency dependent network equivalents for the EMTP," *IEEE Trans. Power Del.*, vol. 8, no. 3, pp. 1402–1412, Jul. 1993.

[8] B. Gustavsen and O. Mo, "Interfacing convolution based linear models to an electromagnetic transients program," presented at the Int. Conf. Power Systems Transients, Lyon, France, Jun. 4–7, 2007.

[9] A. Morched, B. Gustavsen, and M. Tartibi, "A universal model for accurate calculation of electromagnetic transients on overhead lines and underground cables," *IEEE Trans. Power Del.*, vol. 14, no. 3, pp. 1032–1038, Jul. 1999.

[10] V. Q. Do and M. M. Gavrilovic, "An iterative pole removal method for synthesis of power system equivalent networks," *IEEE Trans. Power App. Syst.*, vol. PAS-103, no. 8, pp. 2065–2070, Aug. 1984.

[11] V. Q. Do and M. M. Gavrilovic, "A synthesis method for one-port and multi-port equivalent networks for analysis of power system transients," *IEEE Trans. Power Syst.*, vol. PWRS-1, no. 2, pp. 103–113, Apr. 1986.

[12] B. Gustavsen and A. Semlyen, "Rational approximation of frequency domain responses by vector fitting," *IEEE Trans. Power Del.*, vol. 14, no. 3, pp. 1052–1061, Jul. 1999.

[13] B. Gustavsen, "Computer code for rational approximation of frequency dependent admittance matrices," *IEEE Trans. Power Del.*, vol. 17, no. 4, pp. 1093–1098, Oct. 2002.

[14] B. Gustavsen and A. Semlyen, "Application of vector fitting to state equation representation of transformers for simulation of electromagnetic transients," *IEEE Trans. Power Del.*, vol. 13, no. 3, pp. 834–842, Jul. 1998.

[15] S. Boyd and L. O. Chua, "On the passivity criterion for LTI n-ports," *Circuit Theory App.*, vol. 10, pp. 323–333, 1982.

[16] S. Boyd, L. E. Ghaoui, E. Feron, and V. Balakrishnan, Linear matrix inequalities in system and control theory, SIAM, Singapore, 1994, vol. 15, Studies in applied mathematics. [Online]. Available: http://www.stanford.edu/ boyd/lmibook/

[17] S. Grivet-Talocia, "Passivity enforcement via perturbation of Hamiltonian matrices," *IEEE Trans. Circuits Syst.*, vol. 51, no. 9, pp. 1755–1769, Sep. 2004.

[18] B. Gustavsen, "Fast passivity enforcement for pole-residue models by perturbation of residue matrix eigenvalues," *IEEE Trans. Power Del.*, vol. 23, no. 4, pp. 2278–2285, Oct. 2008.

[19] B. Gustavsen and A. Semlyen, "Enforcing passivity for admittance matrices approximated by rational functions," *IEEE Trans. Power Syst.*, vol. 16, no. 1, pp. 97–104, Feb. 2001.

[20] D. Deschrijver, B. Gustavsen, and T. Dhaene, "Advancements in iterative methods for rational approximation in the frequency domain," *IEEE Trans. Power Del.*, vol. 22, no. 3, pp. 1633–1642, Jul. 2007.

[21] B. Gustavsen and C. Heitz, "Fast realization of the modal vector fitting method for rational modeling with accurate representation of small eigenvalues," *IEEE Trans. Power Del.*, vol. 24, no. 3, pp. 1396–1405, Jul. 2009.

[22] M. Abdel-Rahman, A. Semlyen, and M. R. Iravani, "Two-layer network equivalent for electromagnetic transients," *IEEE Trans. Power Del.*, vol. 18, no. 4, pp. 1328–1335, Oct. 2003.

[23] X. Nie and V. Dinavahi, "A robust two-layer network equivalent for transient studies," in *Proc. Int. Conf. Power System Transients*, Montreal, QC, Canada, Jun. 2005, pp. 1–6.

[24] X. Nie, Y. Chen, and V. Dinavahi, "Real-time transient simulation based on a robust two-layer network equivalent," *IEEE Trans. Power Syst.*, vol. 22, no. 4, pp. 1771–1781, Nov. 2007.

[25] M. Matar and R. Iravani, "A modified multi-port two-layer network equivalent for the analysis of electromagnetic transients," *IEEE Trans. Power Del.*, vol. 25, no. 1, pp. 177–186, Jan. 2010.

[26] J. Graimger and W. D. Stevenson, *Power System Analysis*. New York: McGraw-Hill, 1994.

[27] EMTDC User's Guide. Winnipig, MB, Canada, Manitoba HVDC Res. Ctr., 2004.

[28] J. R. Marti, "Accurate modeling of frequency-dependent transmission lines in electromagnetic transient simulations," *IEEE Trans. Power App. Syst.*, vol. PAS-101, no. 1, pp. 147–157, Jan. 1982.

[29] M. Matar and R. Iravani, "FPGA implementation of a modified two-layer network equivalent for real-time simulation of electromagnetic transients," presented at the IPST, Kyoto, Japan, Jun. 2009.

[30] A. Semlyen and M. R. Iravani, "Frequency domain modeling of external systems in an electro-magnetic transients program," *IEEE Trans. Power Syst.*, vol. 8, no. 2, pp. 527–533, May 1993.

[31] L. Pak, M. O. Faruque, X. Nie, and V. Dinavahi, "A versatile cluster-based real-time digital simulator for power engineering research," *IEEE Trans. Power Syst.*, vol. 21, no. 2, pp. 455–465, May 2006.

[32] J. R. Marti, "Accurate modeling of frequency-dependent transmission lines in electromagnetic transient simulations," *IEEE Trans. Power App. Syst.*, vol. PAS-101, no. 1, pp. 147–155, Jan. 1982.

[33] J. Reeve and R. Adapa, "A new approach to dynamic analysis of AC networks incorporating detailed modeling of DC systems. I. Principles and implementation," *IEEE Trans. Power Del.*, vol. 3, no. 4, pp. 2005–2011, Oct. 1988.

[34] R. Adapa and J. Reeve, "A new approach to dynamic analysis of AC networks incorporating detailed modeling of DC systems. II. Application to interaction of DC and weak AC systems," *IEEE Trans. Power Del.*, vol. 3, no. 4, pp. 2012–2019, Oct. 1988.

[35] A. M. Stankovic and T. Aydin, "Analysis of asymmetrical faults in power systems using dynamic phasors," *IEEE Trans. Power Syst.*, vol. 15, no. 3, pp. 1062–1068, Aug. 2000.

[36] A. M. Stankovic, S. R. Sanders, and T. Aydi, "Dynamic phasors in modeling and analysis of unbalanced polyphase AC machines," *IEEE Trans. Energy Convers.*, vol. 17, no. 1, pp. 107–113, Mar. 2002.

[37] E. Davison, "A method for simplifying linear dynamic systems," *IEEE Trans. Autom. Control*, vol. 11, no. 1, pp. 93–101, Jan. 1966.

[38] J. M. Undrill and A. E. Turner, "Construction of power system electromechanical equivalents by modal analysis," *IEEE Trans. Power App. Syst.*, vol. PAS-90, no. 5, pp. 2049–2059, Sep. 1971.

[39] J. H. Chow, *Time Scale Modelling of Dynamic Networks with Applications to Power Systems*. New York: Springer-Verlag, 1982.

[40] I. J. Perez-Arriaga, "Selective modal analysis with applications to electric power systems," Ph.D. dissertation, Electrical Eng., Mass. Inst. Technol., Cambridge, MA , 1981.

[41] I. J. Perez-Arriaga, G. C. Verghese, and F. C. Schweppe, "Selective modal analysis with application to electric power systems, Part I: Heuristic Introduction," *IEEE Trans. Power App. Syst.*, vol. PAS-101, no. 9, pp. 3117–3125, Sep. 1982.

[42] I. J. Perez-Arriaga, G. C. Verghese, and F. C. Schweppe, "Selective modal analysis with application to electric power systems, Part II: The Dynamic Stability Problem," *IEEE Trans. Power App. Syst.*, vol. PAS-101, no. 9, pp. 3126–3134, Sep. 1982.

[43] H. Y. Altalib and P. C. Krause, "Dynamic equivalents by combination of reduced order models of system components," *IEEE Trans. Power App. Syst.*, vol. PAS-95, no. 5, pt. 1, pp. 1535–1544, Sep. 1976.

[44] S. E. M. de Oliveira and A. G. Massaud, "Modal dynamic equivalent for electric power systems I: Theory," *IEEE Trans. Power Syst.*, vol. 3, no. 4, pp. 1731–1737, Nov. 1988.

[45] S. E. M. de Oliveira and A. G. Massaud, "Modal dynamic equivalent for electric power systems. II: Stability simulation tests," *IEEE Trans. Power Syst.*, vol. 3, no. 4, pp. 1731–1737, Nov. 1988.

[46] G. Troullinos, J. F. Dorsey, H. Wong, J. Myers, and S. Goodwin, "Estimating order reduction for dynamic equivalents," *IEEE Trans. Power App. Syst.*, vol. PAS-104, no. 12, pp. 3475–3481, Dec. 1985.

[47] R. Nath and S. S. Lamba, "Development of coherency-based time-domain equivalent model using structure constraints," *Proc. Inst. Elect. Eng., Gen., Transm. Distrib.*, vol. 133, no. 4, pp. 165–175, May 1986.

[48] M. L. Ourari, L.-A. Dessaint, and V.-Q. Do, "Dynamic equivalent modeling of large power systems using structure preservation technique," *IEEE Trans. Power Syst.*, vol. 21, no. 3, pp. 1284–1295, Aug. 2006.

[49] R. J. Galarza, J. H. Chow, W. W. Price, A. W. Hargrave, and P. M. Hirsch, "Aggregation of exciter models for constructing power system dynamic equivalents," *IEEE Trans. Power Syst.*, vol. 13, no. 3, pp. 782–788, Aug. 1998.

[50] R. J. Newell, M. D. Risan, L. Allen, I. S. Rao, and D. L. Stuehm, "Utility experience with coherency-based dynamic equivalents of very large systems," *IEEE Trans. Power App. Syst.*, vol. PAS-104, no. 11, pp. 3056–3063, Nov. 1985.

[51] L. Wang, M. Klein, S. Yirga, and P. Kundur, "Dynamic reduction of large power systems for stability studies," *IEEE Trans. Power Syst.*, vol. 12, no. 2, pp. 889–895, May 1997.

[52] X. Lei, D. Povh, and O. Ruhle, "Industrial approaches for dynamic equivalents of large power systems," in *Proc. IEEE Power Eng. Soc. Winter Meeting*, 2002, pp. 1036–1042.

[53] A. J. Germond and R. Podmore, "Dynamic aggregation of generating unit models," *IEEE Trans. Power App. Syst.*, vol. PAS-97, no. 4, pp. 1060–1069, Jul. 1978.

[54] "Dynamic reduction, Final report," EPRI, EPRI TR-102234, Project 2447-01, 1993, vol. 1.

[55] W. W. Price, A. W. Hargrave, J. H. Chow, B. J. Hurysz, and P. M. Hirsch, "Large-scale system testing of a power system dynamic equivalencing program," *IEEE Trans. Power Syst.*, vol. 13, no. 3, pp. 768–74, Aug. 1998.

[56] S. B. Yusof, G. J. Rogers, and R. T. H. Alden, "Slow coherency based network partitioning including load buses," *IEEE Trans. Power Syst.*, vol. 8, no. 3, pp. 1375–1382, Aug. 1993.

[57] S. Geeves, "A modal-coherency technique for deriving dynamic equivalents," *IEEE Trans. Power Syst.*, vol. 3, no. 1, pp. 44–51, Feb. 1988.

[58] R. Nath, S. S. Lamba, and K. S. Prakasa Rao, "Coherency based system decomposition into study and external areas using weak coupling," *IEEE Trans. Power App. Syst.*, vol. PAS-104, no. 6, pp. 1443–1449, Jun. 1985.

[59] Y.-N. Yu and M. A. El-Sharkawi, "Estimation of external dynamic equivalents of a thirteen-machine system," *IEEE Trans. Power App. Syst.*, vol. PAS-100, no. 3, pp. 1324–1332, Mar. 1981.

[60] A. M. Stankovic and A. T. Saric, "Transient power system analysis with measurement-based gray box and hybrid dynamic equivalents," *IEEE Trans. Power Syst.*, vol. 19, no. 1, pp. 455–462, Feb. 2004.

[61] P. Ju, L. Q. Ni, and F. Wu, "Dynamic equivalents of power systems with online measurements. Part 1: Theory," *Proc. Inst. Elect. Eng., Gen., Transm. Distrib.*, vol. 151, no. 2, pp. 175–178, Mar. 2004.

[62] P. Ju, F. Li, N. G. Yang, X. M. Wu, and N. Q. He, "Dynamic equivalents of power systems with online measurements Part 2: Applications," *Proc. Inst. Elect. Eng., Gen., Transm. Distrib.*, vol. 151, no. 2, pp. 179–182, Mar. 2004.

[63] X. Lin, A. M. Gole, and M. Yu, "A wide-band multi-port system equivalent for real time digital power system simulators," *IEEE Trans. Power Syst.*, vol. 24, no. 1, pp. 237–249, Feb. 2009.

[64] Y. Liang, L. Xi, A. M. Gole, and M. Yu, "Improved coherency-based wide-band equivalents for real time digital simulators," *IEEE Trans. Power Syst.*, vol. 26, no. 3, pp. 1410–1417, Aug. 2011.